ORGANOMETALLICS

pubs.acs.org/Organometallics Article

Silane Activation with Cobalt on the POCOP Pincer Ligand Platform

Yingze Li, Jeanette A. Krause, and Hairong Guan*

Cite This: *Organometallics* 2020, 39, 3721−3730 Read Online

ACCESS | Metrics & More | Article Recommendations | Supporting Information

ABSTRACT: Cobalt POCOP pincer complexes $\{\kappa^P,\kappa^C,\kappa^P\text{-}2,6\text{-}(^i\mathrm{Pr_2PO})_2\mathrm{C_6H_3}\}\mathrm{Co}(\mathrm{PMe_3})_2$ (**1**) and $\{\kappa^P,\kappa^C,\kappa^P\text{-}2,6\text{-}(^i\mathrm{Pr_2PO})_2\text{-}4\text{-}\mathrm{NMe_2}\text{-}\mathrm{C_6H_2}\}\mathrm{Co}(\mathrm{PMe_3})_2$ (**2**) have been synthesized via C−H bond activation of the pincer ligands with $\mathrm{HCo}(\mathrm{PMe_3})_4$. Silanes such as $\mathrm{PhSiH_3}$, $\mathrm{Ph_2SiH_2}$, and $(\mathrm{EtO})_3\mathrm{SiH}$ can undergo Si−H oxidative addition with these Co(I) complexes, though reversibly. One of the silane activation products, namely, $\{\kappa^P,\kappa^C,\kappa^P\text{-}2,6\text{-}(^i\mathrm{Pr_2PO})_2\mathrm{C_6H_3}\}\mathrm{Co}(\mathrm{H})(\mathrm{SiH_2Ph})(\mathrm{PMe_3})$ (**3**), has been isolated and shown to eliminate $\mathrm{PhSiH_3}$ upon evaporation to form $\{\kappa^P,\kappa^C,\kappa^P\text{-}2,6\text{-}(^i\mathrm{Pr_2PO})_2\mathrm{C_6H_3}\}\mathrm{Co}(\mathrm{PMe_3})$ (**4**). Under heating, redistribution of $\mathrm{PhSiH_3}$ in **3** can take place, resulting in $\{\kappa^P,\kappa^C,\kappa^P\text{-}2,6\text{-}(^i\mathrm{Pr_2PO})_2\mathrm{C_6H_3}\}\mathrm{Co}(\mathrm{H})(\mathrm{SiH_3})(\mathrm{PMe_3})$ (**5**) and $\mathrm{Ph_2SiH_2}$. Complexes **1**−**3** have been established as catalysts for the hydrosilylation of aldehydes bearing various functional groups. According to the mechanistic studies, the silyl hydride species exists in the catalytic cycle, whereas the bis(trimethylphosphine) species sits outside the catalytic cycle. Dissociation of $\mathrm{PMe_3}$ is required prior to aldehyde insertion into the silyl hydride species, which is the turnover-limiting step of the catalytic cycle. Consequently, **3** outperforms **1** in catalyzing the hydrosilylation reaction due to the presence of only one $\mathrm{PMe_3}$ ligand. The structures of **1**−**4** have been studied by X-ray crystallography.

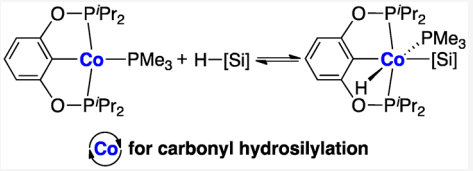

INTRODUCTION

Pincer complexes derived from diphosphinites, or better known as POCOP pincer complexes, have been the subject of extensive studies for almost two decades, largely propelled by their potential to catalyze a broad range of chemical transformations.[1] Iridium POCOP pincer complexes, in particular, are among the most effective catalysts for transfer dehydrogenation of alkanes.[2] The analogous rhodium complexes are versatile catalysts promoting various cross-coupling reactions.[3] The success of these catalytic systems is made possible by the high thermal stability of the pincer framework and the facile two-electron processes occurring at the metal centers (i.e., oxidative addition and reductive elimination reactions).

The advantages of using the POCOP pincer ligand platform could be even more pronounced in the cobalt system, considering that cobalt complexes without tight chelation and strong-field ligands are more prone to decomposition as well as one-electron pathways.[4] However, the chemistry of cobalt POCOP pincer complexes has not been explored until recently. The very first example was reported in 2009 by Li and co-workers, who used $\mathrm{MeCo}(\mathrm{PMe_3})_4$ to activate the central C−H bond of $\mathrm{Ph_2PO(CH_2)_3OPPh_2}$, resulting in the formation of $\{\kappa^P,\kappa^C,\kappa^P\text{-}(\mathrm{Ph_2PO})_2\mathrm{C_3H_5}\}\mathrm{Co}(\mathrm{PMe_3})_2$.[5] This strategy has been extended to the synthesis of other cobalt POCOP pincer complexes, although the phosphorus substituents are limited to phenyl groups.[6] The *tert*-butyl derivatives can be accessed from $\{\kappa^P,\kappa^C,\kappa^P\text{-}2,6\text{-}(^t\mathrm{Bu_2PO})_2\mathrm{C_6H_3}\}\mathrm{CoI}$, which is available via lithiation of $1,3\text{-}(^t\mathrm{Bu_2PO})_2\text{-}2\text{-}\mathrm{I}\text{-}\mathrm{C_6H_3}$, followed by the addition of $\mathrm{CoI_2}\cdot\mathrm{THF}$.[7] The analogous precursor $\{\kappa^P,\kappa^C,\kappa^P\text{-}2,6\text{-}(^i\mathrm{Pr_2PO})_2\mathrm{C_6H_3}\}\mathrm{CoCl}$ has been made through cyclometalation of $1,3\text{-}(^i\mathrm{Pr_2PO})_2\mathrm{C_6H_4}$ with $\mathrm{CoCl_2}$ assisted by 4-dimethylaminopyridine.[8] While these studies have focused on stoichiometric reactions, oxidative addition of $\mathrm{CH_3I}$[5] and $\mathrm{H_2}$[7a] and reductive elimination of two aryl groups[8] have been established, showing promise for catalysis involving a Co(I)/Co(III) cycle.

We have recently reported the synthesis of $\{\kappa^P,\kappa^C,\kappa^P\text{-}2,6\text{-}(\mathrm{Ph_2PO})_2\mathrm{C_6H_3}\}\mathrm{Co(CO)_2}$, $\{\kappa^P,\kappa^C,\kappa^P\text{-}2,6\text{-}(^t\mathrm{Bu_2PO})_2\mathrm{C_6H_3}\}\mathrm{Co(CO)}$, and $\{\kappa^P,\kappa^C,\kappa^P\text{-}2,6\text{-}(^i\mathrm{Pr_2PO})_2\text{-}4\text{-}\mathrm{R}\text{-}\mathrm{C_6H_2}\}\mathrm{Co(CO)_2}$ via ligand C−H bond activation with $\mathrm{Co_2(CO)_8}$.[9] These carbonyl complexes are active catalysts for the hydrosilylation of aldehydes. However, the catalytic reactions are best carried out in an open system, which allows the dissociated CO to escape from the reaction vessel.[9a] This complicates the NMR studies of the mechanism. In addition, the presence of the π-accepting CO ligand is likely to disfavor an oxidative addition process[7b] that might be needed for silane activation. We have thus shifted our attention to cobalt POCOP pincer complexes free of CO. In this paper, we first describe a new method of activating diphosphinite C−H bonds with cobalt. The resulting cobalt POCOP pincer complexes prove to be improved hydrosilylation catalysts. Our mechanistic study sheds light on how silanes are activated at the cobalt center, including the characterization of silane oxidative addition products.

Received: August 19, 2020
Published: October 7, 2020

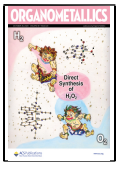

https://dx.doi.org/10.1021/acs.organomet.0c00553
Organometallics 2020, 39, 3721−3730

RESULTS AND DISCUSSION

Synthesis of Co(I) Complexes. Inspired by the work of Li and Sun,[5,6] we first attempted to use $Co(PMe_3)_4$ and $MeCo(PMe_3)_4$ to activate POCOP pincer ligands bearing isopropyl groups as the phosphorus substituents. Treatment of 1,3-$(^iPr_2PO)_2C_6H_4$ with $Co(PMe_3)_4$ failed to produce any pincer complexes. The reaction with $MeCo(PMe_3)_4$ showed some success in forming the desired product $\{\kappa^P,\kappa^C,\kappa^P$-2,6-$(^iPr_2PO)_2C_6H_3\}Co(PMe_3)_2$ (**1**) but suffered from reproducibility issues, likely due to the difficulty in obtaining pure $MeCo(PMe_3)_4$.[10] We then turned to another low-valent cobalt precursor $HCo(PMe_3)_4$, which can be more readily synthesized through $NaBH_4$ reduction of $Co(acac)_2$ in the presence of PMe_3.[11] The anticipated C−H bond activation process took place at 80 °C, converting 1,3-$(^iPr_2PO)_2C_6H_4$ to **1** (eq 1),

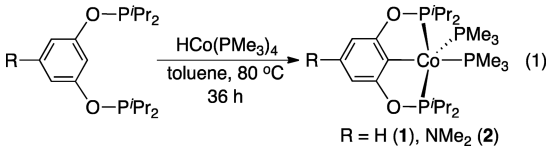

which was isolated as a red powder in 66% yield. A similar procedure applied to 1,3-$(^iPr_2PO)_2$-5-NMe_2-C_6H_3 and $HCo(PMe_3)_4$ led to the isolation of $\{\kappa^P,\kappa^C,\kappa^P$-2,6-$(^iPr_2PO)_2$-4-$NMe_2$-$C_6H_2\}Co(PMe_3)_2$ (**2**) in 60% yield.

Both Co(I) complexes were found to be highly air-sensitive; upon brief exposure to air (<5 min), the solid samples changed color from red to black and became viscous. Under an inert atmosphere, they can be stored for months without noticeable degradation. Saturated pentane solutions kept in a glovebox freezer (−30 °C) produced dark red crystals suitable for X-ray crystallographic studies (Figures 1 and 2). One notable feature

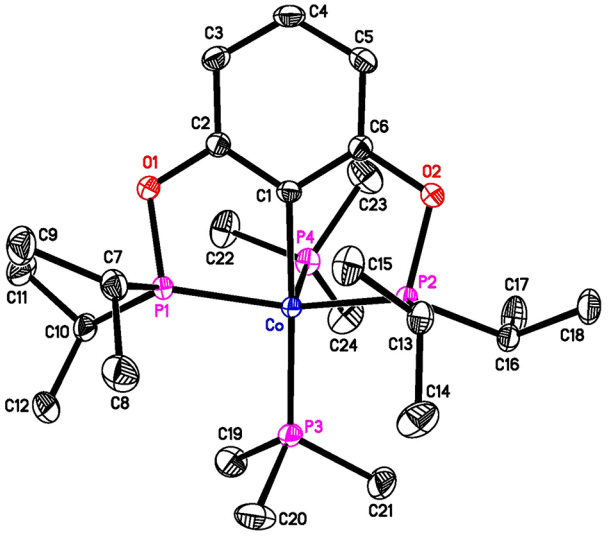

Figure 1. ORTEP drawing of $\{\kappa^P,\kappa^C,\kappa^P$-2,6-$(^iPr_2PO)_2C_6H_3\}Co(PMe_3)_2$ (**1**) crystallized in the monoclinic space group $P2_1/n$ (50% probability level, hydrogen atoms omitted for clarity). Selected bond lengths (Å) and angles (deg): Co−C(1) 1.9560(11), Co−P(1) 2.1642(3), Co−P(2) 2.1604(3), Co−P(3) 2.1903(3), Co−P(4) 2.2228(3); C(1)−Co−P(1) 77.54(3), C(1)−Co−P(2) 78.53(3), P(1)−Co−P(2) 135.467(13), C(1)−Co−P(3) 175.23(3), C(1)−Co−P(4) 85.89(3), P(1)−Co−P(3) 99.977(12), P(2)−Co−P(3) 100.855(12), P(1)−Co−P(4) 104.406(12), P(2)−Co−P(4) 110.700(12), P(3)−Co−P(4) 98.711(13).

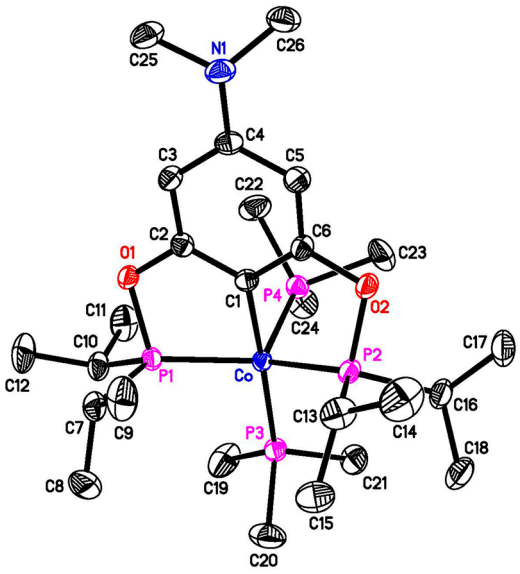

Figure 2. ORTEP drawing of $\{\kappa^P,\kappa^C,\kappa^P$-2,6-$(^iPr_2PO)_2$-4-$NMe_2$-$C_6H_2\}Co(PMe_3)_2$ (**2**) at the 50% probability level (hydrogen atoms omitted for clarity). Selected bond lengths (Å) and angles (deg): Co−C(1) 1.9569(17), Co−P(1) 2.1516(5), Co−P(2) 2.1695(5), Co−P(3) 2.1806(5), Co−P(4) 2.2221(5); C(1)−Co−P(1) 78.16(5), C(1)−Co−P(2) 77.52(5), P(1)−Co−P(2) 135.07(2), C(1)−Co−P(3) 175.93(5), C(1)−Co−P(4) 85.83(5), P(1)−Co−P(3) 100.20(2), P(2)−Co−P(3) 101.42(2), P(1)−Co−P(4) 110.88(2), P(2)−Co−P(4) 104.36(2), P(3)−Co−P(4) 98.24(2).

of the structures is a severe distortion of the pincer arms away from PMe_3, as reflected by a relatively small P(1)−Co−P(2) angle [**1**: 135.467(13)°; **2**: 135.07(2)°]. For comparison, the corresponding P−Co−P angles for the dicarbonyl complexes $\{\kappa^P,\kappa^C,\kappa^P$-2,6-$(^iPr_2PO)_2C_6H_3\}Co(CO)_2$ [155.024(13)°] and $\{$2,6-$(^iPr_2PO)_2$-4-NMe_2-$C_6H_2\}Co(CO)_2$ [151.68(4)° and 155.51(4)° for two independent molecules] are ∼20° wider and more coplanar with the pincer backbone.[9a] The related $\{\kappa^P,\kappa^C,\kappa^P$-2,6-$(^iPr_2PO)_2C_6H_3\}Fe(PMe_3)_2H$ also displays a wider P−M−P angle of 143.73(3)° formed by the POCOP pincer ligand.[12] Geometry indices[13] calculated for both structures (**1**: τ = 0.66; **2**: τ = 0.68) suggest that the coordination geometry about cobalt is best described as distorted trigonal bipyramidal with the *ipso* carbon and a PMe_3 ligand occupying the axial positions.

Solution structures of **1** and **2** (in C_6D_6) probed by NMR spectroscopy further confirmed that the two PMe_3 ligands are not related by symmetry. Two different sets of PMe_3 resonances were observed in the ^1H, $^{13}C\{^1H\}$, and $^{31}P\{^1H\}$ NMR spectra, and two methine resonances of the isopropyl groups were also located in each $^{13}C\{^1H\}$ NMR spectrum. These results are in contrast to our previous NMR studies of the dicarbonyl complexes $\{\kappa^P,\kappa^C,\kappa^P$-2,6-$(^iPr_2PO)_2C_6H_3\}Co(CO)_2$ and $\{\kappa^P,\kappa^C,\kappa^P$-2,6-$(^iPr_2PO)_2$-4-$NMe_2$-$C_6H_2\}Co(CO)_2$, which exhibit C_{2v} symmetry in solution.[9a] For reasons unclear to us, the phosphorus-carbon coupling is better resolved for **1**, displaying a doublet at 35.0 ppm (J = 21.9 Hz) and a triplet at 33.4 ppm (J = 9.2 Hz). These ^{13}C resonances are assigned to the *cis* and *trans* methine carbons (relative to the equatorial PMe_3), respectively, under the assumption that Karplus-type correlation can be extended to vicinal $^{31}P-^{13}C$ coupling involving a P−Co−P−C connectivity.[14] According to the solid-state structure (Figure 1), the *cis* methine carbons C(10) and C(16) form dihedral angles of 56.31(5)° and 52.71(5)°

https://dx.doi.org/10.1021/acs.organomet.0c00553
Organometallics 2020, 39, 3721−3730

with P(4) through a Co−P bond, consistent with a negligible vicinal coupling constant. A more significant $^3J_{P\text{-}C}$ value is expected for the *trans* methine carbons C(7) and C(13), as suggested by the P(4)−Co−P−C dihedral angles of 159.80(5)° and 169.62(5)°. It is worth noting that, due to strongly coupled *trans* phosphorus nuclei, [2,6-(^{i}Pr$_2$PO)$_2$C$_6$H$_3$]-ligated cobalt pincer complexes often show a "virtually coupled" triplet for the isopropyl methine carbons.[8,9] The absence of virtual coupling in **1** is quite unusual but in agreement with its solid-state structure, illustrating that the POCOP phosphorus atoms are no longer strictly *trans* to each other.

Both Co(I) complexes were characterized by elemental analysis, and compound **1** was further studied by electrospray ionization mass spectrometry (ESI-MS). The measured mass of the $[M + H]^+$ ion at m/z 553.2086 (5%) is consistent with the molecular mass for **1**. The more intense peaks at m/z 476.1565 (100%) and m/z 492.1511 (26%) correspond to $[M - PMe_3]^+$ and $[M - PMe_3 + O]^+$ ions, respectively, suggesting that PMe_3 dissociation and oxidation of the cobalt complex are facile under mass spectral conditions.

Catalytic Studies. We previously reported that the dicarbonyl complex {$\kappa^P,\kappa^C,\kappa^P$-2,6-(^{i}Pr$_2$PO)$_2C_6H_3$}Co(CO)$_2$ catalyzed the hydrosilylation of PhCHO with (EtO)$_3$SiH at 50 °C to yield (EtO)$_3$SiOCH$_2$Ph, though only in a vessel connected to an argon-filled Schlenk line.[9a] With a catalyst loading of 1 mol %, the reaction was complete in 24 h. When performed in a sealed NMR tube, a much higher temperature (>100 °C) was needed, resulting in multiple products. The bis(trimethylphosphine) complexes reported here not only display higher catalytic efficiencies but also avoid the need for an open system. As shown in Table 1 (entry 1), by using **1** to catalyze the same hydrosilylation process, the catalyst loading can be lowered to 0.5 mol % and the reaction time can be shortened to 3 h. However, the hydrosilylation reaction is accompanied by alkoxide exchange on silicon to give rise to a mixture of (EtO)$_n$Si(OCH$_2$Ph)$_{4-n}$ (n = 0−3).[15] The dimethylamine-substituted compound **2** is a more active catalyst, requiring only 1.5 h to fully reduce PhCHO (entry 2). Replacing (EtO)$_3$SiH with other silanes such as Ph$_2$SiH$_2$ (entry 3) and PhSiH$_3$ (entry 4) is feasible. The former was shown to convert PhCHO to Ph$_2$SiH(OCH$_2$Ph)[16] as the sole product, whereas the use of PhSiH$_3$ led to a 37:59:4 mixture of PhSiH$_2$(OCH$_2$Ph), PhSiH(OCH$_2$Ph)$_2$, and PhSi(OCH$_2$Ph)$_3$.[15b,17] By contrast, Ph$_3$SiH, PhMe$_2$SiH, and Et$_3$SiH are not viable silanes under the catalytic conditions, showing no conversion of PhCHO and no hydrosilylation products (entries 5−7). In our experience with catalytic hydrosilylation of aldehydes, acid impurities can sometimes shut down the reaction, as demonstrated in the catalytic system based on {$\kappa^P,\kappa^C,\kappa^P$-2,6-(^{i}Pr$_2$PO)$_2C_6H_3$}NiH.[18] This is not a concern for the cobalt system; using an undistilled sample of PhCHO containing ~3 mol % PhCO$_2$H had a minimum impact on the efficiency and yield (entry 8).

Substrate scope of the catalytic system was examined using **2** as the catalyst and (EtO)$_3$SiH as the silane. The hydrosilylation reactions were performed at 50 °C in sealed J. Young NMR tubes and monitored every 3 h by ^{1}H NMR spectroscopy. As illustrated in Table 2, various functional groups including OMe, NMe$_2$, F, Cl, CF$_3$, NO$_2$, pyrrolyl, thienyl, furyl, and pyridyl groups can be tolerated under the catalytic conditions. Compared to PhCHO, benzaldehyde substituted by *p*-NMe$_2$, *p*-Cl, *p*-NO$_2$, or *o*-Me group as well as 2-naphthaldehyde reacted more slowly. Heterocyclic aldehydes such as pyrrole-2-carboxaldehyde and 2-thiophenecarboxaldehyde also proved to be less reactive, presumably due to their abilities to bind cobalt through the heteroatoms. Blocking the nitrogen site with a methyl group (pyrrole-2-carboxaldehyde → *N*-methyl-2-pyrrolecarboxaldehyde) or replacing sulfur with the less donating oxygen (2-thiophenecarboxaldehyde → furfural)

Table 1. Cobalt-Catalyzed Hydrosilylation of PhCHO with Various Silanes[a]

PhCHO + H−[Si] —(0.5 mol% [Co], C$_6$D$_6$, 50 °C)→ PhCH$_2$O−[Si]

entry	[Co]	silane	time (h)	NMR conversion (%)[b]	NMR yield (%)[b]
1	**1**	(EtO)$_3$SiH	3	>99	>99[c]
2	**2**	(EtO)$_3$SiH	1.5	>99	>99[c]
3	**2**	Ph$_2$SiH$_2$	1.5	>99	>99
4	**2**	PhSiH$_3$	1.5	>99	>99[c]
5	**2**	Ph$_3$SiH	15	0	0
6	**2**	PhMe$_2$SiH	15	0	0
7	**2**	Et$_3$SiH	15	0	0
8[d]	**2**	(EtO)$_3$SiH	1.5	>99	98[c]

[a]Conditions: PhCHO (1.0 mmol), silane (1.2 mmol), cobalt catalyst (0.0050 mmol), and hexamethylbenzene (0.050 mmol, internal standard) mixed with 300 μL of C$_6$D$_6$ in a sealed J. Young NMR tube, 50 °C. [b]Determined by ^{1}H NMR spectroscopy. [c]Multiple hydrosilylation products were present. [d]Undistilled PhCHO with ~3 mol % of the aldehyde oxidized to PhCO$_2$H.

Table 2. Hydrosilylation of Aldehydes or Ketones Catalyzed by 2[a]

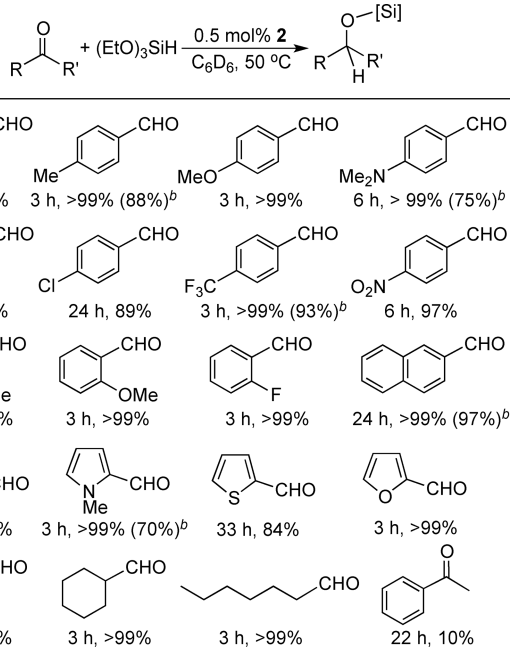

[a]Conditions: RCOR′ (1.0 mmol), (EtO)$_3$SiH (1.2 mmol), and **2** (0.0050 mmol) mixed with 300 μL of C$_6$D$_6$ in a sealed J. Young NMR tube, 50 °C. Numbers listed are reaction time and percentage conversion of RCOR′ (determined by ^{1}H NMR spectroscopy). [b]Number given in parentheses is the isolated yield for the alcohol obtained from hydrolysis of the silyl ether products.

https://dx.doi.org/10.1021/acs.organomet.0c00553
Organometallics 2020, 39, 3721−3730

resulted in a faster hydrosilylation process. To our surprise, the pyridine ring in 2-pyridinecarboxaldehyde did not appear to inhibit the catalysis. Aliphatic aldehydes such as cyclohexanecarboxaldehyde and heptanal underwent smooth hydrosilylation reaction with $(EtO)_3SiH$. However, reduction of ketones was ineffective, as indicated by a low conversion of acetophenone over an extended period of time.

Overall, **2** showed substantially higher catalytic efficiencies than the dicarbonyl complex $\{\kappa^P,\kappa^C,\kappa^P\text{-}2,6\text{-}(^iPr_2PO)_2\text{-}4\text{-}NMe_2\text{-}C_6H_2\}Co(CO)_2$, but lower selectivities for $(EtO)_3SiOCHRR'$ because of the more prevalent alkoxide exchange process. In fact, substrates in Table 2 all led to 2−4 hydrosilylation products. However, hydrolysis of the initially formed silyl ethers with a 10% aqueous solution of NaOH allowed the isolation of pure R′RCHOH in modest to high yield, as demonstrated in a number of select examples (Table 2).

Silane Activation. The hydrosilylation of PhCHO with $(EtO)_3SiH$ in C_6D_6 catalyzed by **1** or **2** (1 mol %) could take place at room temperature, albeit slowly, reducing 58% or 88% of PhCHO, respectively, over a period of 20 h. Monitoring the catalytic process by $^{31}P\{^1H\}$ NMR spectroscopy revealed a new pincer complex (with **1**: 213.3 and 2.9 ppm; with **2**: 213.1 and 3.8 ppm) along with the starting bis(trimethylphosphine) complex. The resonances of the new species integrated in a 2:1 ratio, suggesting that only one PMe_3 ligand was left on cobalt.

The subsequent mechanistic study was focused on **1**, especially to identify the new pincer complex observed during the catalytic reaction. A solution of **1** in C_6D_6 was first treated with 1 equiv of PhCHO, which did not yield any new product after 24 h. In contrast, the 1:1 mixture of **1** and $(EtO)_3SiH$ in C_6D_6 immediately generated that species with two phosphorus resonances at 213.3 and 2.9 ppm, which accounted for ∼3% of total pincer complexes. The amount was increased to 43% when 100 equiv of $(EtO)_3SiH$ was added. The most characteristic proton resonance was a doublet of triplets at −14.26 ppm (J = 78.0 and 61.6 Hz), indicative of forming a cobalt hydride. This splitting pattern, coupled with the observation of free PMe_3 (δ_P = −61.4 ppm), is consistent with an oxidative addition product arising from $(EtO)_3SiH$ and $\{\kappa^P,\kappa^C,\kappa^P\text{-}2,6\text{-}(^iPr_2PO)_2C_6H_3\}Co(PMe_3)$.

Silanes that failed to reduce PhCHO under our catalytic conditions (i.e., Ph_3SiH, $PhMe_2SiH$, and Et_3SiH) did not react with **1**. The stoichiometric reaction between Ph_2SiH_2 and **1** formed a detectable but negligible amount of a silane activation product. Increasing the Ph_2SiH_2-to-**1** ratio to 100:1 led to 34% conversion of **1** to a new compound, which exhibited spectroscopic features similar to the one generated from the $(EtO)_3SiH$ reaction. On the basis of these results, one might already surmise that only silanes with a small steric profile could undergo oxidative addition to cobalt. Consistent with this hypothesis, 1.5 equiv of $PhSiH_3$ was found sufficient to fully convert **1** to $\{\kappa^P,\kappa^C,\kappa^P\text{-}2,6\text{-}(^iPr_2PO)_2C_6H_3\}Co(H)(SiH_2Ph)(PMe_3)$ (**3**).

After some reaction optimization, **3** was eventually isolated as a yellow solid on a preparative scale involving the addition of 3 equiv of $PhSiH_3$ to **1** dissolved in Et_2O (eq 2). The

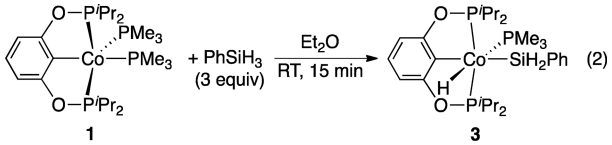

presence of excess $PhSiH_3$ was critical to inhibiting reductive elimination of the silane from **3** (vide infra) during workup, a phenomenon that was previously noted for *trans*-(^{tBu}PNP)-$CoH_2(SiH_2Ph)$ (^{tBu}PNP = 2,6-(di-*tert*-butylphosphinomethyl)-pyridine).[19] The ^1H NMR spectrum of **3** in C_6D_6 displayed a hydride resonance at −14.47 ppm as a doublet of triplets (J = 78.8 and 63.2 Hz) and a SiH_2 resonance at 5.01 ppm as another doublet of triplets (J = 10.0 and 8.0 Hz). The phosphorus resonances were located at 211.9 and −2.6 ppm as two broad peaks for the POCOP pincer ligand and PMe_3, respectively. Unlike **1**, the isopropyl methine carbons of **3** appeared as two triplets of doublets at 35.2 (J = 9.9 and 3.7 Hz) and 33.2 ppm (J = 14.1 and 8.9 Hz) due to virtual coupling to the two POCOP phosphorus nuclei and coupling to the PMe_3 phosphorus nucleus.

The structure of **3** was more firmly established by X-ray crystallography. As shown in Figure 3, cobalt is situated in an

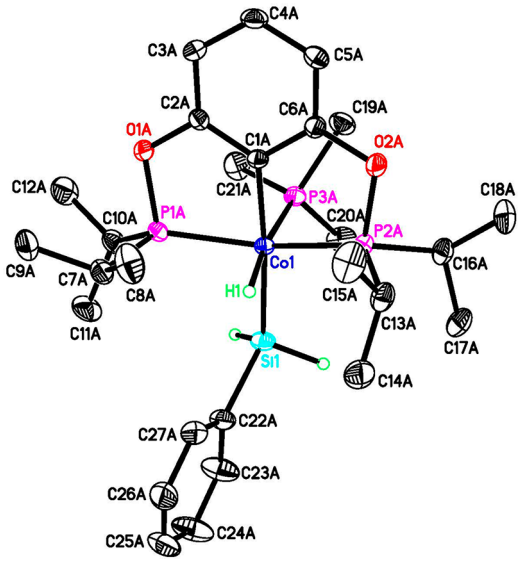

Figure 3. ORTEP drawing of $\{\kappa^P,\kappa^C,\kappa^P\text{-}2,6\text{-}(^iPr_2PO)_2C_6H_3\}Co(H)(SiH_2Ph)(PMe_3)$ (**3**) at the 50% probability level (hydrogen atoms except the ones on Co and Si omitted for clarity, only molecule A shown). Selected bond lengths (Å) and angles (deg): Co(1)−C(1A) 1.9597(12), Co(1)−H(1) 1.42(2), Co(1)−P(1A) 2.1630(4), Co(1)−P(2A) 2.1596(4), Co(1)−P(3A) 2.2343(4), Co(1)−Si(1) 2.2743(4); C(1A)−Co(1)−P(1A) 79.28(4), C(1A)−Co(1)−P(2A) 80.81(4), P(1A)−Co(1)−P(2A) 152.515(15), C(1A)−Co(1)−P(3A) 90.70(4), C(1)−Co(1)−Si(1) 175.44(4), P(1A)−Co(1)−P(3A) 103.289(14), P(2A)−Co(1)−P(3A) 95.690(14), P(1A)−Co(1)−Si(1) 96.158(15), P(2A)−Co(1)−Si(1) 103.466(15), P-(3A)−Co(1)−Si(1) 90.457(14).

octahedral coordination environment with the hydride *trans* to PMe_3 and the SiH_2Ph group *trans* to the *ipso* carbon. Compared to **1**, the pincer arms in **3** are distorted to a lesser extent from the ideal meridional geometry with a significantly wider P−Co−P angle (152.515(15)° vs 135.467(13)° in **1**).[20] The Co−Si bond in **3** (2.2743(4) Å)[21] is 0.04−0.05 Å longer than that in *trans*-(^{tBu}PNP)$CoH_2(SiH_2Ph)$ (2.234(1) and 2.223(1) Å for two independent molecules),[19] likely as a result of having a more *trans*-influencing donor opposite to the SiH_2Ph site.

Interestingly, the solution of **3** in C_6D_6 changed color over time from yellow to blue. Evaporation of a pentane solution that was prefiltered through a pad of Celite or a PTFE syringe

https://dx.doi.org/10.1021/acs.organomet.0c00553
Organometallics 2020, 39, 3721−3730

filter resulted in a blue solid. The SiH_2Ph and hydride resonances were absent from the ^1H NMR spectrum of the isolated product (in C_6D_6), implying that elimination of $PhSiH_3$ from cobalt had occurred. Additional evidence supporting the formula $\{\kappa^P,\kappa^C,\kappa^P\text{-}2,6\text{-}(^iPr_2PO)_2C_6H_3\}Co(PMe_3)$ (**4**) included the increased symmetry as judged by ^1H and $^{13}C\{^1H\}$ NMR spectroscopy and the observation of two phosphorus resonances at 208.3 and −10.5 ppm, which integrated in a 2:1 ratio. Recrystallization of **4** from Et_2O-pentane at −30 °C produced two different dichroic crystals—one dark green-purple and one dark blue-red. The former were analyzed as the expected 4-coordinate Co(I) complex featuring a square planar coordination geometry (Figure 4). The Co−P

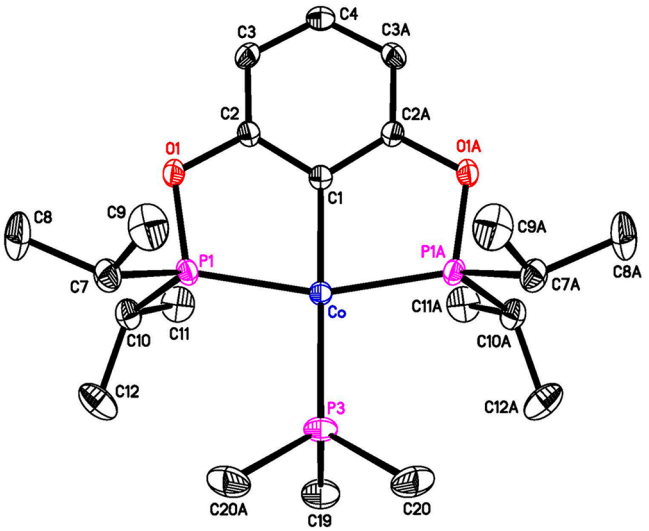

Figure 4. ORTEP drawing of $\{\kappa^P,\kappa^C,\kappa^P\text{-}2,6\text{-}(^iPr_2PO)_2C_6H_3\}Co(PMe_3)$ (**4**) at the 50% probability level (hydrogen atoms omitted for clarity). Selected bond lengths (Å) and angles (deg): Co−C(1) 1.942(3), Co−P(1) and Co−P(1A) 2.1459(5), Co−P(3) 2.1748(8); C(1)−Co−P(1) and C(1)−Co−P(1A) 80.504(14), P(1)−Co−P(1A) 161.01(3), C(1)−Co−P(3) 178.93(9), P(1)−Co−P(3) and P(1A)−Co−P(3) 99.493(14).

bonds are ∼0.02 Å shorter than the corresponding bonds in $\{\kappa^P,\kappa^C,\kappa^P\text{-}2,6\text{-}(^iPr_2PO)_2C_6H_3\}Co(PMe_3)_2$ (**1**), and the pincer core in **4** is considerably flat in comparison to **1** and **3**. The dark blue-red dichroic crystals solve as **1** but crystallized in the monoclinic space *Pn* rather than the monoclinic space group $P2_1/n$ as the structure shown in Figure 1 (see Supporting Information for details). This result is consistent with the fact that **4** is unstable even under an inert atmosphere. Decomposition of **4** likely released PMe_3, which in turn bound to **4** to form the more stable bis(trimethylphosphine) complex **1**.

Si−H bond activation with a low-valent cobalt species is an established strategy for the synthesis of PSiP pincer complexes.[22] Simple silanes like $PhSiH_3$ often add oxidatively to Co(I) in a *reversible* fashion,[19,23] similar to what we

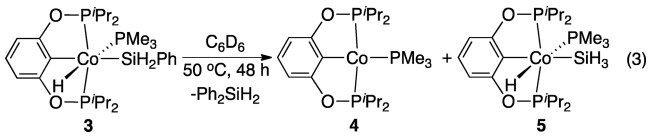

(3)

observed with **1**. Unexpectedly, another reaction outcome was noticed when the oxidative addition product **3** was heated to 50 °C (eq 3). After 48 h, in addition to **4** (∼20%), which resulted from reductive elimination of $PhSiH_3$, a new cobalt pincer complex **5** emerged from the reaction mixture (∼30%). This new species displayed a silyl proton resonance at 3.80 ppm as a doublet of triplets (J = 11.6 and 5.2 Hz) with ^{29}Si satellites ($^1J_{Si\text{-}H}$ = 156.0 Hz) and a hydride resonance at −14.52 ppm also as doublet of triplets (J = 86.4 and 61.2 Hz). Apart from the pincer complexes, Ph_2SiH_2 was found in the ^1H NMR spectrum (5.08 ppm, $^1J_{Si\text{-}H}$ = 198.4 Hz), prompting us to propose that **5** was most likely $\{\kappa^P,\kappa^C,\kappa^P\text{-}2,6\text{-}(^iPr_2PO)_2C_6H_3\}Co(H)(SiH_3)(PMe_3)$ generated via redistribution of $PhSiH_3$.[24] The chemical shift value of 3.80 ppm is in agreement with those reported for other $MSiH_3$ complexes.[25] Zuzek and Parkin recently showed an analogous reaction involving the conversion of $(Me_3P)_4Mo(SiH_2Ph)_2H_2$ and $PhSiH_3$ to $(Me_3P)_4Mo(SiH_2Ph)(SiH_3)H_2$, $(Me_3P)_4Mo(SiH_3)_2H_2$, and Ph_2SiH_2,[26] and proposed a metathesis of Mo−SiH_2Ph and Ph−SiH_3 bonds.[27] It is possible that such a mechanism is also operative here following the dissociation of PMe_3. Attempts to isolate **5** for further characterization were unsuccessful. The spatial arrangement of the hydride, SiH_3, and PMe_3 was assigned based on the similarity of the hydride resonances between **3** and **5**; having a hydride and a silyl group *trans* to each other, for example, would shift the hydride resonance to a more upfield region (e.g., −5.5 to −7.5 ppm in a CCC pincer system[28]). The observation of **5** at 50 °C suggested that, at that temperature, **5** might participate in the catalytic cycle. However, it can only be a minor pathway, because the conversion of **3** to **5** is significantly slower than the reduction of aldehydes with **3**.

Mechanistic Consideration. Complex **3** is more likely involved in the main catalytic cycle when $PhSiH_3$ is employed as the silane. To probe its ability to reduce aldehydes, a C_6D_6 solution of **3** was treated with PhCHO in consecutive additions. The reaction was fast at room temperature, reaching completion in a few minutes. The first equivalent of PhCHO consumed ∼50% of **3** to give rise to **4** along with a minor product **6** (<5%) that featured a hydride resonance at −14.36 ppm (doublet of triplets, J = 77.6 and 64.0 Hz). The organic products were identified as $PhSiH(OCH_2Ph)_2$ and $PhSi(OCH_2Ph)_3$ in a 13:1 ratio. The amount of $PhSiH_2(OCH_2Ph)$ was negligible, indicating that, during the hydrosilylation process, $PhSiH_2(OCH_2Ph)$ was more reactive than $PhSiH_3$. Adding the second equivalent of PhCHO led to the disappearance of **3** but the formation of **1** (10%), **4** (70%), and some pincer degradation products. The ratio between $PhSiH(OCH_2Ph)_2$ and $PhSi(OCH_2Ph)_3$ decreased to 1.1:1. As

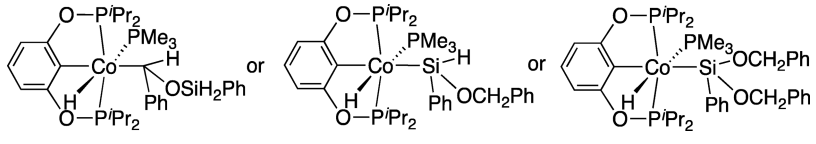

Figure 5. Plausible structures of **6**.

https://dx.doi.org/10.1021/acs.organomet.0c00553
Organometallics 2020, 39, 3721−3730

expected, adding the third equivalent of PhCHO depleted all available Si−H bonds to yield $PhSi(OCH_2Ph)_3$ almost exclusively. The pincer complexes consisted of **1**, **4**, pincer degradation products, and a new hydride species **7** (<5%) signaled by a triplet at −11.85 ppm (J = 44.8 Hz). Due to the minute amounts of **6** and **7** generated during the reaction and the fleeting nature of **6**, identifying the exact structures of these two cobalt hydrides was difficult. On the basis of the available spectroscopic data, **6** could be a complex resulting from PhCHO insertion into the Co−Si bond of **3** or oxidative addition of $PhSiH_2(OCH_2Ph)$ (or $PhSiH(OCH_2Ph)_2$) to **4** (Figure 5). Hydride **7** lacked PMe_3 as the ancillary ligand and could be the result of C−H bond activation of $PhSi(OCH_2Ph)_3$ with a highly reactive intermediate $\{\kappa^P,\kappa^C,\kappa^P\text{-}2,6\text{-}(^iPr_2PO)_2C_6H_3\}Co$,[29] which might form during the degradation of **4**. The major pathway, as summarized in Scheme 1,

Scheme 1. Major Pathway for the Hydrosilylation of PhCHO with 3

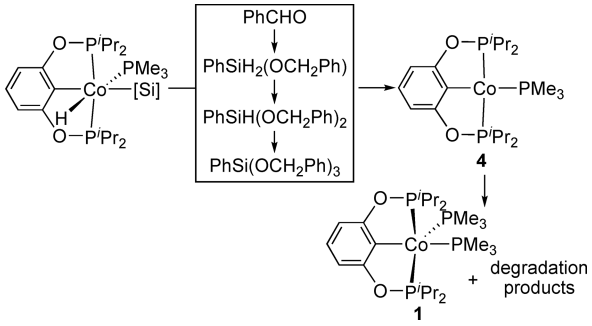

involves iterative hydrosilylation steps (i.e., Si−H oxidative addition, carbonyl insertion, and reductive elimination of a silyl ether) of PhCHO with all Si−H bonds originated from $PhSiH_3$. When the reaction arrives at the $PhSiH(OCH_2Ph)_2$ stage, Si−H oxidative addition with **4** becomes less favorable, thereby increasing the likelihood of **4** scavenging any dissociated PMe_3 to form **1** with concomitant degradation of $\{\kappa^P,\kappa^C,\kappa^P\text{-}2,6\text{-}(^iPr_2PO)_2C_6H_3\}Co$.

Compound **3** is an 18-electron complex, and its reaction with PhCHO is likely to proceed via prior dissociation of PMe_3. Studying the direct impact of added PMe_3 on the reduction of PhCHO by **3** was, however, impeded by the competing conversion of **3** to **1**. As mentioned earlier, the silane activation process is reversible. Mixing an equimolecular amount of **1** and $PhSiH_3$ in C_6D_6 generated **3** in situ (84% conversion) along with the release of PMe_3 (Scheme 2). At room temperature, adding 1 equiv of PhCHO (with respect to total cobalt species) to this mixture afforded a very small amount of hydrosilylation products over several hours, contrasting to the fast reaction between pure **3** and PhCHO. However, raising the temperature to 50 °C resulted in a nearly

Scheme 2. Reaction of in Situ Generated 3 with PhCHO

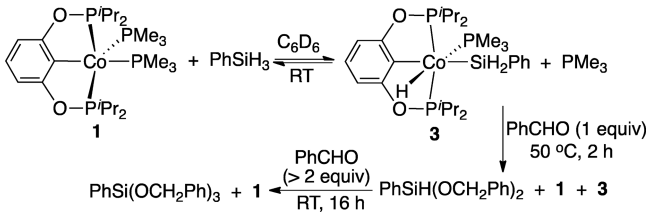

quantitative conversion of PhCHO to $PhSiH(OCH_2Ph)_2$ within 2 h. The cobalt pincer complexes present in the reaction mixture were **1** and **3** (~50% each). Further addition of PhCHO (>3 equiv total) provided $PhSi(OCH_2Ph)_3$ cleanly as the final hydrosilylation product and recovered **1** almost fully. Overall, these results suggest that PMe_3 plays an inhibitory role in reducing aldehydes but at the same time stabilizes the pincer complexes.

Both **1** and **3** were studied as catalysts for room-temperature hydrosilylation of PhCHO with $(EtO)_3SiH$ (Figure 6).

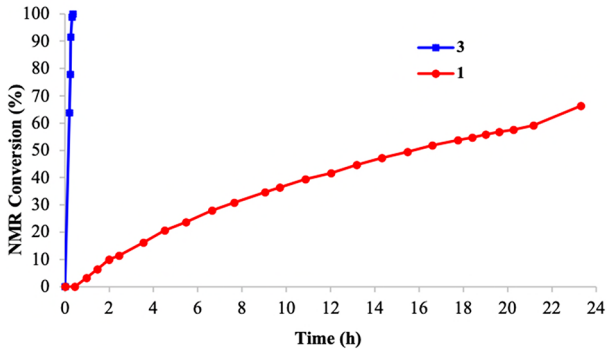

Figure 6. Conversion of PhCHO as a function of time (reaction conditions: 1.0 mmol of PhCHO, 1.1 mmol of $(EtO)_3SiH$, 1 mol % catalyst, and 0.050 mmol of hexamethylbenzene mixed in 250 μL of C_6D_6, 23 °C).

Consistent with the stoichiometric studies described above (though involving $PhSiH_3$), the catalytic reaction with **3** (1 mol %) was significantly faster, requiring as short as 20 min to fully convert PhCHO to the hydrosilylation products. The reaction catalyzed by **1**, however, showed an induction period of ~30 min, possibly for the time needed to accumulate an appreciable amount of the catalytically active species $\{\kappa^P,\kappa^C,\kappa^P\text{-}2,6\text{-}(^iPr_2PO)_2C_6H_3\}Co(H)\{Si(OEt)_3\}(PMe_3)$ (**8**).

The silane activation product **8** was observed from the reaction of **1** with $(EtO)_3SiH$, although the equilibrium lies heavily to the bis(trimethylphosphine) complex side. It was, however, the dominant species when **4** was mixed with excess $(EtO)_3SiH$ (eq 4). To probe its role in the catalytic cycle, the

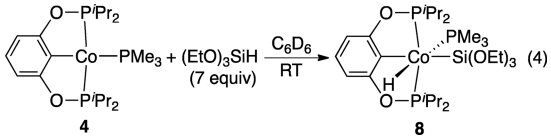

reactions shown in Figure 6 were monitored by $^{31}P\{^1H\}$ NMR spectroscopy. For the reaction catalyzed by **3**, **8** was the only observable cobalt species, confirming that **8** was the resting state of the catalyst. In contrast, for the reaction catalyzed by **1**, both **1** and **8** (in comparable quantities) were observed throughout the productive stage of the catalytic process.

A catalytic mechanism consistent with our experimental data is outlined in Scheme 3. When the bis(trimethylphosphine) complex **1** catalyzes the hydrosilylation reaction, only a fraction of the cobalt species enters into the catalytic cycle, in the form of a cobalt silyl hydride like **8**. The subsequent reduction of PhCHO, which is the turnover-limiting step of the catalytic cycle, requires the dissociation of PMe_3. Carbonyl insertion into the Co−Si bond is expected to generate a siloxyalkyl intermediate,[30] although we cannot rule out the possibility of

https://dx.doi.org/10.1021/acs.organomet.0c00553
Organometallics 2020, 39, 3721−3730

Scheme 3. Catalytic Cycle Proposed for 1-Catalyzed Hydrosilylation of PhCHO with $(EtO)_3SiH$

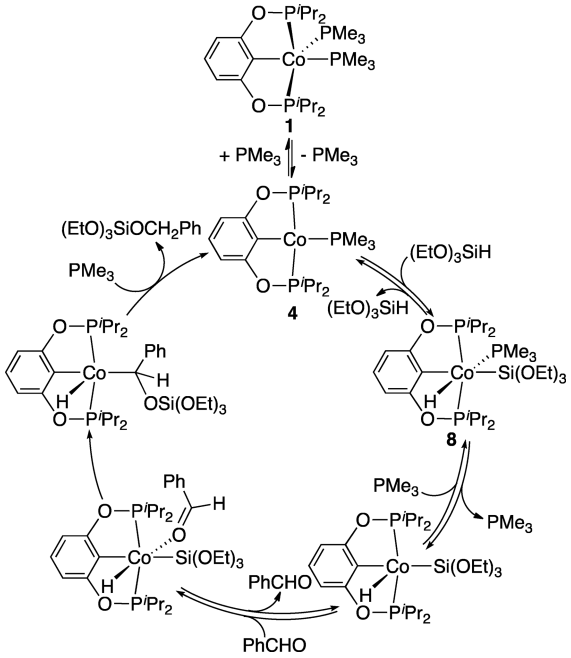

carbonyl insertion into the Co−H bond.[31] In any case, reductive elimination of the silyl ether product and coordination of PMe_3 closes the catalytic cycle by regenerating **4**. Catalytic hydrosilylation of aldehydes with $PhSiH_3$ proceeds via a similar pathway, except that the silyl ether products can undergo further reaction, owing to the multiple Si−H bonds. Bulkyl silanes such as Ph_3SiH, $PhMe_2SiH$, Et_3SiH, and $Ph_2SiH(OCH_2Ph)$ (generated from hydrosilylation of PhCHO with Ph_2SiH_2) are unable to reduce aldehydes due to their difficulty in forming the cobalt silyl hydride intermediates. Hydrosilylation of PhCHO with $(EtO)_3SiH$ catalyzed by **3** starts with aldehyde reduction with the activated $PhSiH_3$, which eventually forms **4** and then uses $(EtO)_3SiH$ to turn the catalytic cycle over. Under such a scenario, all cobalt species exist in their productive form and the amount of free PMe_3 present in the solution is too small to exert the inhibitory effect, which explains a much faster catalytic reaction with **3** (Figure 6).

CONCLUSIONS

In this work, we have developed a new synthetic route to cobalt POCOP pincer complexes using $HCo(PMe_3)_4$ to activate the ligand C−H bonds. The resulting Co(I) bis(trimethylphosphine) complexes react reversibly with certain silanes including $PhSiH_3$, Ph_2SiH_2, and $(EtO)_3SiH$ to form Co(III) silyl hydride complexes. One of such Co(III) species, namely, $\{\kappa^P,\kappa^C,\kappa^P\text{-}2,6\text{-}(^iPr_2PO)_2C_6H_3\}Co(H)(SiH_2Ph)(PMe_3)$, is amenable to isolation but gradually loses $PhSiH_3$ to yield $\{\kappa^P,\kappa^C,\kappa^P\text{-}2,6\text{-}(^iPr_2PO)_2C_6H_3\}Co(PMe_3)$. Both the Co(I) bis(trimethylphosphine) complexes and the Co(III) silyl hydride complexes are capable of catalyzing the hydrosilylation of aldehydes, with catalytic efficiencies much higher than those for the previously reported catalysts involving cobalt dicarbonyl complexes.[9a] Our mechanistic investigation suggests that aldehyde insertion into the Co(III) silyl hydride species is the turnover-limiting step, which can be inhibited by PMe_3. Most importantly, we have demonstrated the possibility of performing both oxidative addition and reductive elimination reactions with cobalt on a very popular pincer ligand platform, and we have incorporated these steps into a catalytic process. Our future efforts will be directed to other catalytic transformations that involve a Co(I)/Co(III) cycle.

EXPERIMENTAL SECTION

General Methods. Unless otherwise noted, all organometallic compounds were prepared and handled under an argon atmosphere using standard glovebox and Schlenk techniques. Dry and oxygen-free toluene, diethyl ether, and pentane were collected from an Innovative Technology solvent purification system and used throughout the experiments involving cobalt complexes. Methanol was degassed by bubbling argon through it for 30 min and then dried over 4 Å molecular sieves before use. Benzene-d_6 (99.5% D) was dried over Na-benzophenone and distilled under an argon atmosphere. Benzaldehyde used for catalytic reaction optimization was freshly distilled prior to use. All other carbonyl substrates as well as the solvents for column chromatography were used as received without further purification. $HCo(PMe_3)_4$,[11] 1,3-$(^iPr_2PO)_2C_6H_4$,[32] and 1,3-$(^iPr_2PO)_2$-5-NMe_2-C_6H_3[9a] were prepared as described in the literature. Chemical shift values for ^1H and $^{13}C\{^1H\}$ NMR spectra were referenced internally to the residual solvent resonances. $^{31}P\{^1H\}$ NMR spectra were referenced externally to 85% H_3PO_4 (0 ppm). High-resolution mass spectrometry data were acquired using a Thermo Scientific Orbitrap Fusion Lumos mass spectrometer.

*Synthesis of $\{\kappa^P,\kappa^C,\kappa^P\text{-}2,6\text{-}(^iPr_2PO)_2C_6H_3\}Co(PMe_3)_2$ (**1**).* In a glovebox, 1,3-$(^iPr_2PO)_2C_6H_4$ (775 mg, 2.26 mmol) dissolved in 20 mL of toluene was added dropwise to a Schlenk flask containing a solution of $HCo(PMe_3)_4$ (750 mg, 2.06 mmol) in 15 mL of toluene. The flask was removed from the glovebox, connected to a Schlenk line, and heated while stirring at 80 °C for 36 h, during which time the color of the reaction mixture gradually changed from orange to dark red. After cooling to room temperature, the mixture was filtered into another Schlenk flask via a cannula. The filtrate was concentrated under vacuum to give a reddish oily residue, which was triturated with chilled (0 °C) methanol (0.5 mL × 6). The resulting solid was dried under vacuum to afford the product as a red fine powder (750 mg, 66% yield). ^1H NMR (400 MHz, C_6D_6, δ): 6.88 (t, $J_{H\text{-}H}$ = 7.6 Hz, Ar*H*, 1H), 6.64 (d, $J_{H\text{-}H}$ = 7.6 Hz, Ar*H*, 2H), 2.49−2.30 (m, C*H*$(CH_3)_2$, 4H), 1.59−1.41 (m, CH(C*H*$_3)_2$, 6H), 1.39−1.24 (m, CH(C*H*$_3)_2$, 6H), 1.22−1.01 (m, CH(C*H*$_3)_2$, 12H), 1.15 (d, $J_{P\text{-}H}$ = 6.4 Hz, P(C*H*$_3)_3$, 9H), 0.92 (d, $J_{P\text{-}H}$ = 4.8 Hz, P(C*H*$_3)_3$, 9H). $^{13}C\{^1H\}$ NMR (101 MHz, C_6D_6, δ): 162.6 (t, $J_{P\text{-}C}$ = 8.6 Hz, Ar*C*), 141.3 (br, Ar*C*), 124.2 (s, Ar*C*), 103.8 (t, $J_{P\text{-}C}$ = 4.5 Hz, Ar*C*), 35.0 (d, $J_{P\text{-}C}$ = 21.9 Hz, CH$(CH_3)_2$), 33.4 (t, $J_{P\text{-}C}$ = 9.2 Hz, *C*H$(CH_3)_2$), 26.9 (d, $J_{P\text{-}C}$ = 20.8 Hz, P$(CH_3)_3$), 21.9 (d, $J_{P\text{-}C}$ = 12.8 Hz, P$(CH_3)_3$), 20.0 (s, CH$(CH_3)_2$), 18.9 (s, CH$(CH_3)_2$), 18.5 (s, CH$(CH_3)_2$), 18.0 (s, CH$(CH_3)_2$). $^{31}P\{^1H\}$ NMR (162 MHz, C_6D_6, δ): 201.9 (br, O*P*$^iPr_2$, 2P), 5.5 (br, *P*Me_3, 1P), −17.3 (br, *P*Me_3, 1P). Anal. Calcd for $C_{24}H_{49}O_2P_4Co$: C, 52.18; H, 8.94. Found: C, 51.38; H, 8.89. ESI-MS of **1** in anhydrous MeOH (m/z): $[M + H]^+$ calcd for $C_{24}H_{50}O_2P_4Co$ 553.2088, found 553.2086; $[M - PMe_3 + O]^+$ calcd for $C_{21}H_{40}O_3P_3Co$ 492.1517, found 492.1511; $[M - PMe_3]^+$ calcd for $C_{21}H_{40}O_2P_3Co$ 476.1568, found 476.1565.

*Synthesis of $\{\kappa^P,\kappa^C,\kappa^P\text{-}2,6\text{-}(^iPr_2PO)_2\text{-}4\text{-}NMe_2\text{-}C_6H_2\}Co(PMe_3)_2$ (**2**).* This compound was prepared in 60% yield (as a red powder) from 1,3-$(^iPr_2PO)_2$-5-NMe_2-C_6H_3 and $HCo(PMe_3)_4$ following a procedure similar to that used for **1**. ^1H NMR (400 MHz, C_6D_6, δ): 6.29 (s, Ar*H*, 2H), 2.60 (s, N(C*H*$_3)_2$, 6H), 2.52−2.37 (m, C*H*$(CH_3)_2$, 4H), 1.65−1.42 (m, CH(C*H*$_3)_2$, 6H), 1.41−1.28 (m, CH(C*H*$_3)_2$, 6H), 1.28−1.07 (m, CH(C*H*$_3)_2$, 12H), 1.19 (d, $J_{P\text{-}H}$ = 6.4 Hz, P(C*H*$_3)_3$, 9H), 1.04−0.87 (m, P(C*H*$_3)_3$, 9H). $^{13}C\{^1H\}$ NMR (101 MHz, C_6D_6, δ): 162.8 (br, Ar*C*), 151.2 (s, Ar*C*), 123.2 (br, Ar*C*), 91.3 (s, Ar*C*), 41.3 (s, N(*C*H$_3)_2$), 34.9 (br, *C*H$(CH_3)_2$), 33.4 (br, *C*H$(CH_3)_2$), 27.1 (d, $J_{P\text{-}C}$ = 19.8 Hz, P$(CH_3)_3$), 22.2 (br, P$(CH_3)_3$), 20.2 (s, CH$(CH_3)_2$), 18.9 (s, CH$(CH_3)_2$), 18.7 (s, CH$(CH_3)_2$), 18.1 (s, CH$(CH_3)_2$). $^{31}P\{^1H\}$ NMR (162 MHz, C_6D_6, δ): 200.1 (br, O*P*$^iPr_2$, 2P), 5.6 (br, *P*Me_3, 1P), −17.2 (br, *P*Me_3, 1P). Anal. Calcd for

https://dx.doi.org/10.1021/acs.organomet.0c00553
Organometallics 2020, 39, 3721−3730

$C_{26}H_{54}NO_2P_4Co$: C, 52.44; H, 9.14; N, 2.35. Found: C, 52.58; H, 9.33; N, 2.42.

General Procedure for the Catalytic Hydrosilylation of Aldehydes and Ketones. To a J. Young NMR tube were added a 0.10 M stock solution of **2** (50 μL, 0.0050 mmol) in C_6D_6, a carbonyl substrate (1.0 mmol), $(EtO)_3SiH$ (222 μL, 1.2 mmol), and 250 μL of C_6D_6. The resulting mixture was heated at 50 °C (in an oil bath) and monitored by ^1H NMR spectroscopy. For selected substrates, the reaction was quenched with a 10% aqueous solution of NaOH (∼1.2 mL) and stirred vigorously at 50 °C for 24 h. The organic product was extracted with Et_2O (20 mL × 3), dried over anhydrous $MgSO_4$, and concentrated under vacuum. The residue was further purified by flash column chromatography using 20% ethyl acetate in hexanes as eluent. The ^1H and $^{13}C\{^1H\}$ NMR spectra of the alcohol products are provided in the Supporting Information.

*Synthesis of {κ^P,κ^C,κ^P-2,6-(^{i}Pr$_2$PO)$_2$C$_6$H$_3$}Co(H)(SiH$_2$Ph)(PMe$_3$) (**3**).* In a glovebox, to a solution of **1** (200 mg, 0.36 mmol) in Et_2O (20 mL) was added $PhSiH_3$ (133 μL, 1.08 mmol), resulting in an immediate color change of the reaction mixture from red to orange. After stirring at room temperature for 1 h, the volatiles were removed in vacuo. The resulting yellow solid was redissolved in 10 mL of Et_2O and then passed through a Titan3 PTFE syringe filter. The filtrate was concentrated under vacuum to give the desired product as a yellow solid (160 mg, 76% yield). ^1H NMR (400 MHz, C_6D_6, δ): 8.10 (d, J_{H-H} = 7.6 Hz, Ar*H*, 2H), 7.30 (t, J_{H-H} = 7.2 Hz, Ar*H*, 2H), 7.19 (t, J_{H-H} = 7.2 Hz, Ar*H*, 1H), 6.91 (t, J_{H-H} = 7.6 Hz, Ar*H*, 1H), 6.76 (d, J_{H-H} = 8.0 Hz, Ar*H*, 1H), 5.01 (overlapping dt with ^{29}Si satellites, J_{P-H} = 10.0 and 8.0 Hz, $^1J_{Si-H}$ = 151.6 Hz, Si*H*$_2$Ph, 2H), 2.90−2.65 (m, C*H*(CH$_3$)$_2$, 2H), 2.51−2.18 (m, C*H*(CH$_3$)$_2$, 2H), 1.34−1.07 (m, CH(C*H*$_3$)$_2$, 24H), 0.85 (d, J_{P-H} = 6.8 Hz, P(C*H*$_3$)$_3$, 9H), −14.47 (dt, J_{P-H} = 78.8 and 63.2 Hz, Co*H*, 1H). $^{13}C\{^1H\}$ NMR (101 MHz, C_6D_6, δ): 164.1 (td, J_{P-C} = 8.2 and 3.6 Hz, ArC), 145.5 (d, J_{P-C} = 5.6 Hz, ArC), 143.6−142.7 (m, ArC), 136.8 (s, ArC), 127.5 (s, ArC), 127.5 (s, ArC), 126.0 (d, J_{P-C} = 3.0 Hz, ArC), 104.3 (td, J_{P-C} = 6.4 and 3.4 Hz, ArC), 35.2 (td, J_{P-C} = 9.9 and 3.7 Hz, *C*H(CH$_3$)$_2$), 33.2 (td, J_{P-C} = 14.1 and 8.9 Hz, *C*H(CH$_3$)$_2$), 19.6 (s, P(*C*H$_3$)$_3$), 18.7 (s, CH(*C*H$_3$)$_2$), 18.6 (s, CH(*C*H$_3$)$_2$), 18.4 (s, CH(*C*H$_3$)$_2$), 18.1 (s, CH(*C*H$_3$)$_2$). $^{31}P\{^1H\}$ NMR (162 MHz, C_6D_6, δ): 211.9 (br, O*P*^{i}Pr$_2$, 2P), −2.6 (br, *P*Me$_3$, 1P). Anal. Calcd for $C_{27}H_{48}O_2P_3SiCo$: C, 55.47; H, 8.28. Found: C, 53.84; H, 7.87. Although these results are outside the range reviewed as establishing analytical purity, they are provided to illustrate the best values obtained to date.

*Synthesis of {κ^P,κ^C,κ^P-2,6-(^{i}Pr$_2$PO)$_2$C$_6$H$_3$}Co(PMe$_3$) (**4**).* A small amount of **3** (10 mg, 0.017 mmol) was dissolved in 1−2 mL of pentane and then passed through a Titan3 PTFE syringe filter. The resulting solution was evaporated over a period of 2 h, leaving a blue solid as the desired product (7.3 mg, ∼90% yield). ^1H NMR (400 MHz, C_6D_6, δ): 7.03 (t, J_{H-H} = 7.6 Hz, Ar*H*, 1H), 6.88 (d, J_{H-H} = 7.6 Hz, Ar*H*, 2H), 2.24−2.05 (m, C*H*(CH$_3$)$_2$, 4H), 1.31−1.22 (m, CH(C*H*$_3$)$_2$, 12H), 1.21−1.13 (m, CH(C*H*$_3$)$_2$, 12H), 1.11 (d, J_{P-H} = 5.6 Hz, P(C*H*$_3$)$_3$, 9H). $^{13}C\{^1H\}$ NMR (101 MHz, C_6D_6, δ): 169.5−168.9 (m, ArC), 126.8 (s, ArC), 103.1 (t, J_{P-C} = 6.1 Hz, ArC), 31.5 (t, J_{P-C} = 9.5 Hz, *C*H(CH$_3$)$_2$), 23.5 (d, J_{P-C} = 22.1 Hz, P(*C*H$_3$)$_3$), 19.9 (s, CH(*C*H$_3$)$_2$), 18.2 (s, CH(*C*H$_3$)$_2$). $^{31}P\{^1H\}$ NMR (162 MHz, C_6D_6, δ): 208.0 (br, O*P*^{i}Pr$_2$, 2P), −10.5 (br, *P*Me$_3$, 1P). This compound decomposed quickly even under an inert atmosphere. Therefore, the elemental analysis was not performed.

X-ray Structure Determinations. Single crystals of **1** (crystallized in the monoclinic space group $P2_1/n$) and **2** were obtained from pentane solutions kept at −30 °C. Single crystals of **3** were obtained from a 1:2 mixture of **1** and $PhSiH_3$ dissolved in diethyl ether, which was allowed to evaporate slowly at room temperature. Single crystals of **4** were grown from Et_2O-pentane at −30 °C; during this process, single crystals of **1** were also obtained, which had crystallized in the monoclinic space group *Pn* with 2 independent molecules in the lattice. Crystal data collection and refinement parameters are provided in the Supporting Information. Intensity data were collected at 150 K on a Bruker dual-wavelength microfocus source D8 Venture Photon-II diffractometer with Cu Kα radiation, λ = 1.54178 Å (for **1** grown from Et_2O-pentane), or with Mo Kα radiation, λ = 0.71073 Å (for all other samples). The data frames were processed using the program SAINT. The data were corrected for decay, Lorentz, and polarization effects as well as absorption and beam corrections. The structures were solved by a combination of direct methods and the difference Fourier technique and refined by full-matrix least-squares on F^2 using the SHELX suite of programs. Non-hydrogen atoms were refined with anisotropic displacement parameters. For **3**, H atoms bound to Co and Si were located directly from the difference map and coordinates refined. The remaining H atoms in **3** and other complexes were calculated and treated with a riding model. No solvent of crystallization is present in the lattice for any of the structures. Two independent molecules of **3** were found in the unit cell. Of the two independent molecules of **1** crystallized in the monoclinic space group *Pn*, one has a disordered isopropyl group, which was refined with a two-component disorder model. Crystal structures of **1**−**4** (including two structures for **1**) have been deposited at the Cambridge Crystallographic Data Centre (CCDC) and allocated the deposition numbers CCDC 2024211−2024215.

■ ASSOCIATED CONTENT

Supporting Information

The Supporting Information is available free of charge at https://pubs.acs.org/doi/10.1021/acs.organomet.0c00553.

NMR spectra of the cobalt complexes, NMR spectra of the alcohols isolated from the catalytic reactions, additional experimental details, and X-ray crystallographic information for **1**−**4** (PDF)
Optimized Cartesian coordinates for **1**-$P2_1/n$ (MOL)
Optimized Cartesian coordinates for **1**-*Pn* (MOL)
Optimized Cartesian coordinates for **2** (MOL)
Optimized Cartesian coordinates for **3** (MOL)
Optimized Cartesian coordinates for **4** (MOL)

Accession Codes

CCDC 2024211−2024215 contain the supplementary crystallographic data for this paper. These data can be obtained free of charge via www.ccdc.cam.ac.uk/data_request/cif, or by emailing data_request@ccdc.cam.ac.uk, or by contacting The Cambridge Crystallographic Data Centre, 12 Union Road, Cambridge CB2 1EZ, UK; fax: +44 1223 336033.

■ AUTHOR INFORMATION

Corresponding Author

Hairong Guan − *Department of Chemistry, University of Cincinnati, Cincinnati, Ohio 45221-0172, United States;* orcid.org/0000-0002-4858-3159; Email: hairong.guan@uc.edu

Authors

Yingze Li − *Department of Chemistry, University of Cincinnati, Cincinnati, Ohio 45221-0172, United States*

Jeanette A. Krause − *Department of Chemistry, University of Cincinnati, Cincinnati, Ohio 45221-0172, United States*

Complete contact information is available at: https://pubs.acs.org/10.1021/acs.organomet.0c00553

Notes

The authors declare no competing financial interest.

■ ACKNOWLEDGMENTS

We thank the NSF Chemical Catalysis Program for support of this research project (CHE-1800151) and the NSF MRI Program for support of the instrumentation used in this study, which include a Bruker D8 Venture diffractometer (CHE-1625737) and a Bruker NEO400 MHz NMR spectrometer

(CHE-1726092). We are also grateful to Dr. Stephen Macha (University of Cincinnati) for his assistance with mass spectral analysis.

REFERENCES

(1) (a) Morales-Morales, D. Recent Applications of Phosphinite POCOP Pincer Complexes Towards Organic Transformations. *Mini-Rev. Org. Chem.* **2008**, *5*, 141−152. (b) Selander, N.; Szabó, K. J. Catalysis by Palladium Pincer Complexes. *Chem. Rev.* **2011**, *111*, 2048−2076. (c) Zargarian, D.; Castonguay, A.; Spasyuk, D. M. ECE-Type Pincer Complexes of Nickel. *Top. Organomet. Chem.* **2013**, *40*, 131−174. (d) Murugesan, S.; Kirchner, K. Non-Precious Metal Complexes with an Anionic PCP Pincer Architecture. *Dalton Trans.* **2016**, *45*, 416−439.

(2) (a) Choi, J.; MacArthur, A. H. R.; Brookhart, M.; Goldman, A. S. Dehydrogenation and Related Reactions Catalyzed by Iridium Pincer Complexes. *Chem. Rev.* **2011**, *111*, 1761−1779. (b) Haibach, M. C.; Kundu, S.; Brookhart, M.; Goldman, A. S. Alkane Metathesis by Tandem Alkane-Dehydrogenation-Olefin-Metathesis Catalysis and Related Chemistry. *Acc. Chem. Res.* **2012**, *45*, 947−958. (c) Kumar, A.; Bhatti, T. M.; Goldman, A. S. Dehydrogenation of Alkanes and Aliphatic Groups by Pincer-Ligated Metal Complexes. *Chem. Rev.* **2017**, *117*, 12357−12384.

(3) (a) Timpa, S. D.; Fafard, C. M.; Herbert, D. E.; Ozerov, O. V. Catalysis of Kumada-Tamao-Corriu Coupling by a (P°C^{O}P)Rh Pincer Complex. *Dalton Trans.* **2011**, *40*, 5426−5429. (b) Timpa, S. D.; Pell, C. J.; Zhou, J.; Ozerov, O. V. Fate of Aryl/Amido Complexes of Rhodium(III) Supported by a POCOP Pincer Ligand: C−N Reductive Elimination, *β*-Hydrogen Elimination, and Relavance to Catalysis. *Organometallics* **2014**, *33*, 5254−5262. (c) Timpa, S. D.; Pell, C. J.; Ozerov, O. V. A Well-Defined (POCOP)Rh Catalyst for the Coupling of Aryl Halides with Thiols. *J. Am. Chem. Soc.* **2014**, *136*, 14772−14779.

(4) Arevalo, R.; Chirik, P. J. Enabling Two-Electron Pathways with Iron and Cobalt: From Ligand Design to Catalytic Applications. *J. Am. Chem. Soc.* **2019**, *141*, 9106−9123.

(5) Xu, G.; Sun, H.; Li, X. Activation of sp^3 Carbon−Hydrogen Bonds by Cobalt and Iron Complexes and Subsequent C−C Bond Formation. *Organometallics* **2009**, *28*, 6090−6095.

(6) (a) Huang, S.; Zhao, H.; Li, X.; Wang, L.; Sun, H. Synthesis of [POCOP]-Pincer Iron and Cobalt Complexes *via* C_{sp3}−H Activation and Catalytic Application of Iron Hydride in Hydrosilylation Reactions. *RSC Adv.* **2015**, *5*, 15660−15667. (b) Lian, Z.; Xu, G.; Li, X. [2,6-Bis(diphenylphosphinooxy)phenyl]bis-(trimethylphosphine)cobalt(I). *Acta Crystallogr., Sect. E: Struct. Rep. Online* **2010**, *66*, m636.

(7) (a) Hebden, T. J.; St. John, A. J.; Gusev, D. G.; Kaminsky, W.; Goldberg, K. I.; Heinekey, D. M. Preparation of a Dihydrogen Complex of Cobalt. *Angew. Chem., Int. Ed.* **2011**, *50*, 1873−1876. (b) Guard, L. M.; Hebden, T. J.; Linn, D. E., Jr; Heinekey, D. M. Pincer-Supported Carbonyl Complexes of Cobalt(I). *Organometallics* **2017**, *36*, 3104−3109.

(8) Foley, B. J.; Palit, C. M.; Timpa, S. D.; Ozerov, O. V. Synthesis of (POCOP)Co(Ph)(X) Pincer Complexes and Observation of Aryl−Aryl Reductive Elimination Involving the Pincer Aryl. *Organometallics* **2018**, *37*, 3803−3812.

(9) (a) Li, Y.; Krause, J. A.; Guan, H. Cobalt POCOP Pincer Complexes via Ligand C−H Bond Activation with $Co_2(CO)_8$: Catalytic Activity for Hydrosilylation of Aldehydes in an Open vs a Closed System. *Organometallics* **2018**, *37*, 2147−2158. (b) Li, Y.; Krause, J. A.; Guan, H. POCOP-Type Cobalt and Nickel Pincer Complexes Bearing an Appended Phosphinite Group. *Can. J. Chem.* **2021**.

(10) Synthesis of $MeCo(PMe_3)_4$ is a three-step process: (1) reduction of $CoCl_2$-PMe_3 to $Co(PMe_3)_4$ by sodium amalgam or Mg metal, (2) a comproportionation reaction between $Co(PMe_3)_4$ and $CoCl_2$, in the presence of PMe_3, to yield $ClCo(PMe_3)_3$, and (3) conversion of $ClCo(PMe_3)_3$ to $MeCo(PMe_3)_4$ using MeLi along with PMe_3. For details, see: Klein, H.-F.; Karsch, H. H. Methylkobaltverbindungen mit nicht Chelatisierenden Liganden, I. Methyltetrakis-(trimethy1phosphin)kobalt und seine Derivate. *Chem. Ber.* **1975**, *108*, 944−955.

(11) Ventre, S.; Simon, C.; Rekhroukh, F.; Malacria, M.; Amatore, M.; Aubert, C.; Petit, M. Catalytic Version of Enediyne Cobalt-Mediated Cycloaddition and Selective Access to Unusual Bicyclic Trienes. *Chem. - Eur. J.* **2013**, *19*, 5830−5835.

(12) Bhattacharya, P.; Krause, J. A.; Guan, H. Iron Hydride Complexes Bearing Phosphinite-Based Pincer Ligands: Synthesis, Reactivity, and Catalytic Application in Hydrosilylation Reactions. *Organometallics* **2011**, *30*, 4720−4729.

(13) $\tau = (\beta - \alpha)/60$; β and α are the two greatest bond angles (in degrees) about the cobalt. For a discussion of geometry index, see: Addison, A. W.; Rao, T. N.; Reedijk, J.; van Rijn, J.; Verschoor, G. C. Synthesis, Structure, and Spectroscopic Properties of Copper(II) Compounds Containing Nitrogen−Sulphur Donor Ligands; the Crystal and Molecular Structure of Aqua[1,7-bis(*N*-methylbenzimidazol-2′-yl)-2,6-dithiaheptane]copper(II) Perchlorate. *J. Chem. Soc., Dalton Trans.* **1984**, 1349−1356.

(14) (a) A Karplus-type correlation was found between the $^3J_{P\text{-}C}$ values and the P−O−C−C dihedral angles in nucleotides. For details, see: Davies, D. B.; Sadikot, H. On the Karplus Relation for ^3J(POCC) of Nucleotides. *Org. Magn. Reson.* **1982**, *20*, 180−183. (b) A similar correlation of $^3J_{Pt\text{-}C}$ values with Pt−N−C−C dihedral angles was observed for platinum complexes. For details, see: Pregosin, P. S.; Sze, S. N.; Salvadori, P.; Lazzaroni, R. A ^{13}C- and ^{195}Pt-NMR Study of the Complexes *trans*-$PtCl_2$(amine)(CH_2═CH_2). *Helv. Chim. Acta* **1977**, *60*, 2514−2521.

(15) For NMR data of $(EtO)_nSi(OCH_2Ph)_{4-n}$, see: (a) Peterson, E.; Khalimon, A. Y.; Simionescu, R.; Kuzmina, L. G.; Howard, J. A. K.; Nikonov, G. I. Diversity of Catalysis by an Imido-Hydrido Complex of Molybdenum. Mechanism of Carbonyl Hydrosilylation and Silane Alcoholysis. *J. Am. Chem. Soc.* **2009**, *131*, 908−909. (b) Neary, M. C.; Quinlivan, P. J.; Parkin, G. Zerovalent Nickel Compounds Supported by 1,2-Bis(diphenylphosphino)benzene: Synthesis, Structures, and Catalytic Properties. *Inorg. Chem.* **2018**, *57*, 374−391.

(16) Tsuchido, Y.; Abe, R.; Kamono, M.; Tanaka, K.; Tanabe, M.; Osakada, K. Hydrosilylation of Aromatic Aldehydes and Ketones Catalyzed by Mono- and Tri-nuclear Platinum(0) Complexes. *Bull. Chem. Soc. Jpn.* **2018**, *91*, 858−864.

(17) Ghosh, C.; Mukhopadhyay, T. K.; Flores, M.; Groy, T. L.; Trovitch, R. J. A Pentacoordinate Mn(II) Precatalyst That Exhibits Notable Aldehyde and Ketone Hydrosilylation Turnover Frequencies. *Inorg. Chem.* **2015**, *54*, 10398−10406.

(18) (a) Chakraborty, S.; Krause, J. A.; Guan, H. Hydrosilylation of Aldehydes and Ketones Catalyzed by Nickel PCP-Pincer Hydride Complexes. *Organometallics* **2009**, *28*, 582−586. (b) Eberhardt, N. A.; Wellala, N. P. N.; Li, Y.; Krause, J. A.; Guan, H. Dehydrogenative Coupling of Aldehydes with Alcohols Catalyzed by a Nickel Hydride Complex. *Organometallics* **2019**, *38*, 1468−1478.

(19) Scheuermann, M. L.; Semproni, S. P.; Pappas, I.; Chirik, P. J. Carbon Dioxide Hydrosilylation Promoted by Cobalt Pincer Complexes. *Inorg. Chem.* **2014**, *53*, 9463−9465.

(20) Compound **3** crystallized as two independent molecules in the lattice, and only molecule A is shown here. In molecule B, the P−Co−P angle formed by the pincer ligand is 153.169(15)°.

(21) The Co−Si bond length in molecule B is 2.2730(4) Å.

(22) (a) Wu, S.; Li, X.; Xiong, Z.; Xu, W.; Lu, Y.; Sun, H. Synthesis and Reactivity of Silyl Iron, Cobalt, and Nickel Complexes Bearing a [PSiP]-Pincer Ligand via Si−H Bond Activation. *Organometallics* **2013**, *32*, 3227−3237. (b) Zhang, J.; Foley, B. J.; Bhuvanesh, N.; Zhou, J.; Janzen, D. E.; Whited, M. T.; Ozerov, O. V. Synthesis and Reactivity of Pincer-Type Cobalt Silyl and Silylene Complexes. *Organometallics* **2018**, *37*, 3956−3962.

(23) Rozenel, S. S.; Padilla, R.; Arnold, J. Chemistry of Reduced Monomeric and Dimeric Cobalt Complexes Supported by a PNP Pincer Ligand. *Inorg. Chem.* **2013**, *52*, 11544−11550.

https://dx.doi.org/10.1021/acs.organomet.0c00553
Organometallics 2020, 39, 3721−3730

(24) (a) Castillo, I.; Tilley, T. D. Mechanistic Aspects of Samarium-Mediated σ-Bond Activations of Arene C−H and Arylsilane Si−C Bonds. *J. Am. Chem. Soc.* **2001**, *123*, 10526−10534. (b) Hao, J.; Vabre, B.; Zargarian, D. Reactions of Phenylhydrosilanes with Pincer-Nickel Complexes: Evidence for New Si−O and Si−C Bond Formation Pathways. *J. Am. Chem. Soc.* **2015**, *137*, 15287−15298.
(25) (a) Ebsworth, E. A. V.; Marganian, V. M.; Reed, F. J. S.; Gould, R. O. Platinum Hydrides Containing Silyl or Germyl Ligands. Crystal Structure of *trans*-Hydridosilylbis(tricyclohexylphosphine)platinum-(II). *J. Chem. Soc., Dalton Trans.* **1978**, 1167−1170. (b) Woo, H.-G.; Heyn, R. H.; Tilley, T. D. σ-Bond Metathesis Reactions for d^0 Metal-Silicon Bonds That Produce Zirconocene and Hafnocene Hydrosilyl Complexes. *J. Am. Chem. Soc.* **1992**, *114*, 5698−5707. (c) Luo, X.-L.; Kubas, G. J.; Burns, C. J.; Bryan, J. C.; Unkefer, C. J. The First Transition Metal η^2-SiH_4 Complexes, *cis*-$Mo(\eta^2\text{-}SiH_4)(CO)(R_2PC_2H_4PR_2)_2$, and Unprecedented Tautomeric Equilibrium between an η^2-Silane Complex and a Hydridosilyl Species: A Model for Methane Coordination and Activation. *J. Am. Chem. Soc.* **1995**, *117*, 1159−1160.
(26) Zuzek, A. A.; Parkin, G. Si−H and Si−C Bond Cleavage Reactions of Silane and Phenylsilanes with $Mo(PMe_3)_6$: Silyl, Hypervalent Silyl, Silane, and Disilane Complexes. *J. Am. Chem. Soc.* **2014**, *136*, 8177−8180.
(27) Perutz, R. N.; Sabo-Etienne, S. The σ-CAM Mechanism: σ Complexes as the Basis of σ-Bond Metathesis at Late-Transition-Metal Centers. *Angew. Chem., Int. Ed.* **2007**, *46*, 2578−2592.
(28) Ibrahim, A. D.; Entsminger, S. W.; Zhu, L.; Fout, A. R. A Highly Chemoselective Cobalt Catalyst for the Hydrosilylation of Alkenes using Tertiary Silanes and Hydrosiloxanes. *ACS Catal.* **2016**, *6*, 3589−3593.
(29) Hydride **7** is substrate specific; using *p*-$CF_3C_6H_4CHO$ as the substrate gave a similar but different hydride (−12.10 ppm, triplet, J = 44.4 Hz) at the end of the reaction.
(30) Nesbit, M. A.; Suess, D. L. M.; Peters, J. C. E−H Bond Activations and Hydrosilylation Catalysis with Iron and Cobalt Metalloboranes. *Organometallics* **2015**, *34*, 4741−4752.
(31) Niu, Q.; Sun, H.; Li, X.; Klein, H.-F.; Flörke, U. Synthesis and Catalytic Application in Hydrosilylation of the Complex *mer*-Hydrido(2-mercaptobenzoyl)tris(trimethylphosphine)cobalt(III). *Organometallics* **2013**, *32*, 5235−5238.
(32) Press, L. P.; Kosanovich, A. J.; McCulloch, B. J.; Ozerov, O. V. High-Turnover Aromatic C−H Borylation Catalyzed by POCOP-Type Pincer Complexes of Iridium. *J. Am. Chem. Soc.* **2016**, *138*, 9487−9497.

https://dx.doi.org/10.1021/acs.organomet.0c00553
Organometallics 2020, 39, 3721−3730